Title

A system for simultaneous near-infrared reflectance and transillumination imaging of occlusal carious lesion

Authors

Simon, Jacob C
Darling, Cynthia L
Fried, Daniel

Publication Date

2016-02-29

DOI

10.1117/12.2218656

Peer reviewed

HHS Public Access

Author manuscript

Proc SPIE Int Soc Opt Eng. Author manuscript; available in PMC 2016 March 20.

Published in final edited form as:

Proc SPIE Int Soc Opt Eng. 2016 February 13; 9692: . doi:10.1117/12.2218656.

A system for simultaneous near-infrared reflectance and transillumination imaging of occlusal carious lesions

Jacob C. Simon, **Cynthia L. Darling**, and **Daniel Fried**[•]

University of California, San Francisco, San Francisco, CA 94143-0758

Abstract

Clinicians need technologies to improve the diagnosis of questionable occlusal carious lesions (QOC's) and determine if decay has penetrated to the underlying dentin. Assessing lesion depth from near-infrared (NIR) images holds great potential due to the high transparency of enamel and stain to NIR light at λ=1300–1700-nm, which allows direct visualization and quantified measurements of enamel demineralization. Unfortunately, NIR reflectance measurements alone are limited in utility for approximating occlusal lesion depth >200-μm due to light attenuation from the lesion body. Previous studies sought to combine NIR reflectance and transillumination measurements taken at λ=1300-nm in order to estimate QOC depth and severity. The objective of this study was to quantify the change in lesion contrast and size measured from multispectral NIR reflectance and transillumination images of natural occlusal carious lesions with increasing lesion depth and severity in order to determine the optimal multimodal wavelength combinations for estimating QOC depth. Extracted teeth with varying amounts of natural occlusal decay were measured using a multispectral-multimodal NIR imaging system at prominent wavelengths within the λ=1300–1700-nm spectral region. Image analysis software was used to calculate lesion contrast and area values between sound and carious enamel regions.

Keywords

near-IR imaging; occlusal carries; detection; reflectance; transillumination; multimodal

1. INTRODUCTION

The development of near-IR imaging technologies for the detection of dental carious lesions has resulted in the fabrication and clinical testing of three distinct imaging modalities [1–4]. These three modalities namely, reflectance, interproximal transillumination and occlusal transillumination are built into hand held intraoral probes and acquire high resolution diagnostic images of teeth by capturing light ranging from 1300–1700-nm with an InGaAs camera. Images from this spectral region provide the greatest contrast between sound and carious enamel due to marked changes in the tissues optical properties that occur upon enamel demineralization and because this change is so large, early stages of caries progression are easily detected with near-IR light [5].

[•]daniel.fried@ucsf.edu.

Clinicians need new technologies that not only can identify early stages of dental caries to facilitate preventative treatment, but also measure lesion depth and determine if the dental decay has reached the underlying dentin to justify restoration. This is most important for lesions located on the tooth occlusal (top) surface, so called questionable occlusal carious lesions (QOC's), where conventional diagnostic methods are very poor. Reports from the National Health and Nutritional Survey (NHANES) [6, 7] and Dental Practice-Based Research Network (DPBRN)[8–10] show nearly one third of all patients have a QOC located on a posterior tooth. Using near-IR images to assess lesion depth holds great potential due to the high transparency of enamel and stain to light at λ=1300–1700-nm, which allows direct visualization and quantified measurements of enamel demineralization. Unfortunately, NIR reflectance measurements alone are limited in utility for approximating occlusal lesion depth beyond >200-μm due to light attenuation from the lesion body [11–13]. Previous studies sought to combine NIR reflectance and transillumination measurements taken at λ=1300-nm alone in order to estimate QOC depth and severity and these data showed a correlation between the lesions contrast with depth and lesion area with depth [14, 15].

Recently, multispectral NIR reflectance and transillumination experiments have demonstrated that the tooth appears darker at wavelengths coincident with increased water absorption and multispectral images can be used to produce increased contrast between different tooth structures such as sound enamel and dentin, dental decay and composite restorative materials [16–18]. Combining measurements from different NIR imaging wavelengths and comparing them with concurrent measurements acquired by complementary imaging modalities should provide improved assessment of lesion depth and severity.

The objective of this study was to design and fabricate a new imaging system that combines multispectral near-IR reflectance and occlusal transillumination imaging modalities into a single device specifically for the detection of QOC's.

2. MATERIALS AND METHODS

2.1 Sample Preparation

Posterior teeth were selected with sound or demineralized occlusal grooves/surfaces for participation in this study. Teeth were collected from patients in the San Francisco Bay area with approval from the UCSF Committee on Human Research. The teeth were sterilized using gamma radiation and stored in 0.1% thymol solution to maintain tissue hydration and prevent bacterial growth.

2.2 NIR Occlusal Transillumination and NIR Cross-Polarized Reflectance

A high sensitivity, InGaAs, SWIR camera (SU640CSX) from Sensors Unlimited (Princeton, NJ), with a 640×512-pixel focal plane array and 12.5-μm pixel pitch was used to capture NIR cross-polarized reflectance and occlusal transillumination images of posterior teeth *in vitro*. Sample images were illuminated with filtered light from two broadband tungsten halogen lamps, Model FOI-1 from E Light Company (Denver, CO) delivered through separate reflectance and transillumination fiber optic cable bundles (Fig. 1). Reflectance

illumination was achieved using a ring light from Volpi (Auburn, NY) equipped with a toroidal NIR linear polarizer custom made from a 3×3-inch polarizing sheet from Edmund Scientific (Barrington, NJ). Occlusal transillumination used a quadfurcated fiber optic bundle to deliver unpolarized light angled apically at the cementoenamel junction from both sides (buccal/lingual) of the tooth. The near-IR camera lens system was equipped with an orthogonal linear polarizer from Thorlabs (Newton, NJ) to produce cross-polarized reflectance images with greatly reduced specular reflection.

The outputs of both broadband light sources were filtered with optical filters housed in a two motorized filter wheels, FW102 from Thorlabs. The reflectance filter wheel contained a short pass 830-nm, band pass 1300-nm and 1460-nm, and long pass 1500-nm filters from Spectragon (Parsippany, NJ). The occlusal transillumination filter wheel contained long pass 1200-nm and 1500-nm filters from Thorlabs. Each filter wheel also contained an aluminum disk used to block the light source providing on/off functionality to the multimodal system. Detailed schematics covering the geometry of each modality and theory of the resulting image contrast can be found in previous publications. A single axis Newport (Irvine, CA) 850G actuator driven by a Newport ESP300 motion controller was utilized to focus each image in the acquisition sequence by moving the camera position. 12-bit image data was delivered over a camera link cable to a Real Time PXIe-1071 chassis with NI-8133 embedded controller and NI-1428 frame grabber from National Instruments (Austin TX). A host computer, Mac Mini 2014 from Apple (Cupertino, CA) running bootcamp and Windows 7 is used to control the Real Time PXIe, both filter wheels and ESP300 motion controller.

3. RESULTS AND DISCUSSION

An *in vitro* multispectral multimodal NIR imaging system was fabricated using the components illustrated in Fig. 1. The imaging system is controlled by a computer network consisting of a host PC and LabView Real Time computer equipped with a camera link frame grabber. Figure 2 is a diagram of the custom LabView host/real time program that synchronizes image acquisition through the real time computer with the changing of imaging wavelength and modalities by the host computer.

The imaging sequence begins with a continuous acquisition of NIR cross polarized reflectance using an 830-nm short pass filter. This spectral region has the greatest scattering coefficient in sound enamel of all other wavelengths detectable by this InGaAs camera and was chosen because of the uniformity of the tooth appearance. The increased scattering at 830-nm results in light reflections localized closer to the surface of the tooth making focusing easier than at other NIR wavelengths. The host computer is used to drive a single-axis linear stage moving the camera into a focused position. After focusing on the sample the image acquisition sequence commences with the push of a button synchronizing the timing between the real time and host computers. The host computer facilitates the switching of NIR filters and imaging modalities in the following order: NIR cross-polarized reflectance at λ=1500–1700-nm, λ=1460-nm, λ=1300 followed by NIR occlusal transillumination at λ=1500–1700-nm and λ=1200–1700-nm.

Live raw and processed images are streamed from the real time computer to the host using a gigabit crossover Ethernet cable and the images are saved onto an external hard drive connected to the real time computer. For each individual image the real time program sets the camera operational settings, acquires the image frames, performs image processing on the raw data, saves the raw and processed measurements, and then communicates to the host computer that imaging was successful using a network published shared variable. Upon receiving communication from the real time computer, the host responds by changing the filter wheels to the next multispectral imaging modality and positions the camera so the next image is in focus.

A major advantage of this multispectral imaging design is that the multispectral-multimodal images are already registered facilitating faster image processing and multispectral pixel by pixel comparison among images. This program relies upon this auto-registration to segregate the tooth surface from its surroundings based on the tooth location measured from the 830-nm image. Due to the high scattering and uniformity of tooth appearance in this spectral region, the image pixel values consistently demonstrate a bimodal distribution in which the tooth is brighter that its surroundings. Figure 3 contains a series of images at multiple stages during the image processes scheme used in this program. First, the raw 830-nm reflectance image (Fig 3-A) is converted into a binary image (Fig. 3-B) by applying a statistical threshold equal to the pixel mean plus 0.33 times the pixel standard deviation. The binary image is then eroded a number of times with a 5×5 hexagonal matrix to remove small bright objects which are not part of the tooth structure followed by a morphological operation to reject border objects without 8-pixel connectivity. To restore the tooth image, the binary undergoes a series of dilations with a 5×5 hexagonal matrix then closed with a 31×31 pixel structuring element. The image is then processed with a Convex Hull procedure which functions to outlines the tooth region by finding the smallest convex set that contains all the points in the processed binary images (Fig. 3-D). The middle left image in figure 3 outlines the pixel region selected by the image processing algorithm on the original image. The final processed binary image is then multiplied with the raw image to remove the background objects from view (Fig. 3-E). The resulting image is then normalized which results in a higher contrast tooth image (Fig. 3-F). With the following multispectral-multimodal images in the sequence preregistered with this initial 830-nm image, the tooth pixel locations are the same and therefore the morphological image from Fig. 3-D can be multiplied by the next raw image in the sequence and normalized very quickly. Figure 4 shows histograms of the pixel values from the raw (top) and processed/normalized (bottom) images found in Fig. 3 Cleaning the image by removing the background and redistributing the pixel values of the bit range will facilitate the use of statistics to aid in the identification of demineralized tooth regions.

This work resulted in an imaging system through which a reliable pixel to pixel comparison of multispectral images is achievable by automatic image registration and focusing. The next phase of this study is to use the multispectral-multimodal images and histological data from tooth occlusal surfaces to build a multiple regression model for predicting lesion depth. This system is also capable of performing angular resolved measurements, which will be investigated for inclusion in the regression model.

Acknowledgments

This work was supported by NIH/NIDCR Grant R01-DE14698.

References

1. Simon JC, Lucas SA, Staninec M, Tom H, Chan KH, Darling CL, Fried D. “Transillumination and reflectance probes for near-IR imaging of dental caries,” Lasers in Dentistry XX. Proc SPIE. 2014; 8929(D):1–6.
2. Fried D, Staninec M, Darling CL, Kang H, Chan K. “In vivo Near-IR Imaging of Occlusal Lesions at 1310-nm,” Lasers in Dentistry XVII. Proc SPIE. 2011; 7884(B):1–7.
3. Staninec M, Douglas SM, Darling CL, Chan K, Kang H, Lee RC, Fried D. Nondestructive Clinical Assessment of Occlusal Caries Lesions using Near-IR Imaging Methods. Lasers Surg Med. 2011; 43(10):951–959. [PubMed: 22109697]
4. Staninec M, Lee C, Darling CL, Fried D. In vivo near-IR imaging of approximal dental decay at 1,310 nm. Lasers Surg Med. 2010; 42(4):292–298. [PubMed: 20432277]
5. Darling CL, Huynh GD, Fried D. Light scattering properties of natural and artificially demineralized dental enamel at 1310 nm. J Biomed Opt. 2006; 11(3):34023. [PubMed: 16822072]
6. Dye B, Thornton-Evans G, Li X, Iafolla T. Dental caries and tooth loss in adults in the United States, 2011–2012. NCHS data brief. 2015; (197):1–8. [PubMed: 25932891]
7. Dye BA, Tan S, Smith V, Lewis BG, Barker LK, Thornton-Evans G, Eke PI, Beltran-Aguilar ED, Horowitz AM, Li CH. Trends in oral health status: United States, 1988–1994 and 1999–2004,” Vital and health statistics. Series 11, Data from the national health survey. 2007; (248):1–92.
8. Makhija SK, Gilbert GH, Funkhouser E, Bader JD, Gordan VV, Rindal DB, Pihlstrom DJ, Qvist V, P. C. G. National Dental. Characteristics, detection methods and treatment of questionable occlusal carious lesions: findings from the national dental practice-based research network. Caries Res. 2014; 48(3):200–207. [PubMed: 24480989]
9. Makhija SK, Gilbert GH, Funkhouser E, Bader JD, Gordan VV, Rindal DB, Qvist V, Norrisgaard P, P. C. G. National Dental. Twenty-month follow-up of occlusal caries lesions deemed questionable at baseline: findings from the National Dental Practice-Based Research Network. J Am Dent Assoc. 2014; 145(11):1112–1118. [PubMed: 25359642]
10. Makhija SK, Gilbert GH, Funkhouser E, Bader JD, Gordan VV, Rindal DB, Bauer M, Pihlstrom DJ, Qvist V, G. National Dental Practice-Based Research Network Collaborative. The prevalence of questionable occlusal caries: findings from the Dental Practice-Based Research Network. J Am Dent Assoc. 2012; 143(12):1343–1350. [PubMed: 23204090]
11. Simon JC, Chan KH, Darling CL, Fried D. Multispectral near-IR reflectance imaging of simulated early occlusal lesions: Variation of lesion contrast with lesion depth and severity. Lasers Surg Med. 2014; 46(3):203–215. [PubMed: 24375543]
12. Chung S, Fried D, Staninec M, Darling CL. “Near infrared imaging of teeth at wavelengths between 1200 and 1600 nm,” Lasers in Dentistry XVII. Proc SPIE. 2011; 7884(X):1–6.
13. Chung S, Fried D, Staninec M, Darling CL. Multispectral near-IR reflectance and transillumination imaging of teeth. Biomed Opt Exp. 2011; 2(10):2804–2814.
14. Lee C, Darling CL, Fried D. “In vitro near-infrared imaging of occlusal dental caries using a germanium enhanced CMOS camera,” Lasers in Dentistry XVI. Proc SPIE. 2010; 7549(K):1–7.
15. Lee C, Lee D, Darling CL, Fried D. Nondestructive assessment of the severity of occlusal caries lesions with near-infrared imaging at 1310 nm. J Biomed Opt. 2010; 15(4):047011–047018. 047011. [PubMed: 20799842]
16. Zakian C, Pretty I, Ellwood R. Near-infrared hyperspectral imaging of teeth for dental caries detection. J Biomed Opt. 2009; 14(6):064047. [PubMed: 20059285]
17. Tom H, Simon JC, Chan KH, Darling CL, Fried D. Near-infrared imaging of demineralization under sealants. J Biomed Opt. 2014; 19(7):77003. [PubMed: 25036214]
18. Simon JC, Lucas S, Lee R, Darling CL, Staninec M, Vanderhobli R, Pelzner R, Fried D. Near-infrared imaging of natural secondary caries,” Lasers in Dentistry XXI. Proc SPIE. 2015; 9306(F): 1–6.

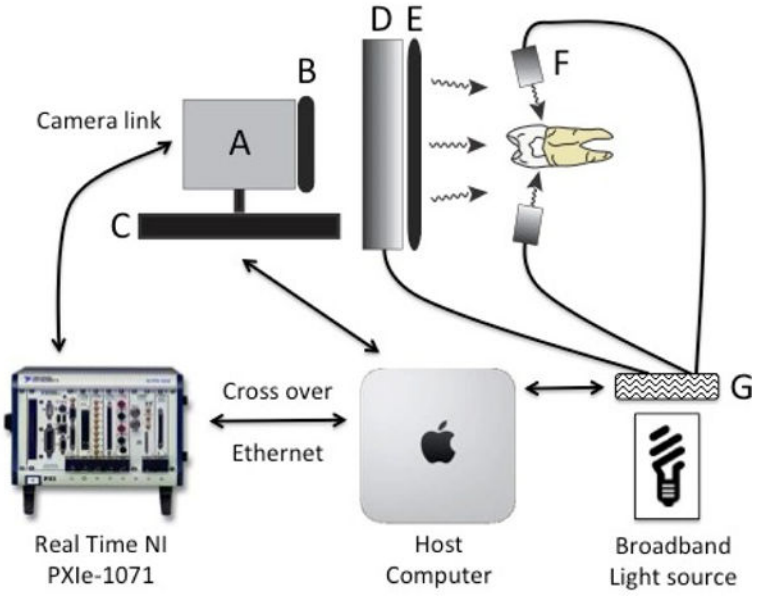

Fig 1.

Imaging schematic for multispectral-multimodal NIR reflectance and occlusal transillumination system. Solid black lines represent fiber optic bundles. Black arrows represent data communication and control. (A) SU640CSX InGaAs NIR camera. (B) NIR linear polarizer. (C) Single axis focusing stage (850G Actuator). (D) Reflectance ring light. (E) Toroidal linear polarizer. (F) Unpolarized occlusal transillumination lights (2 of 4 illustrated). (G) Filter wheel (1 of 2 illustrated).

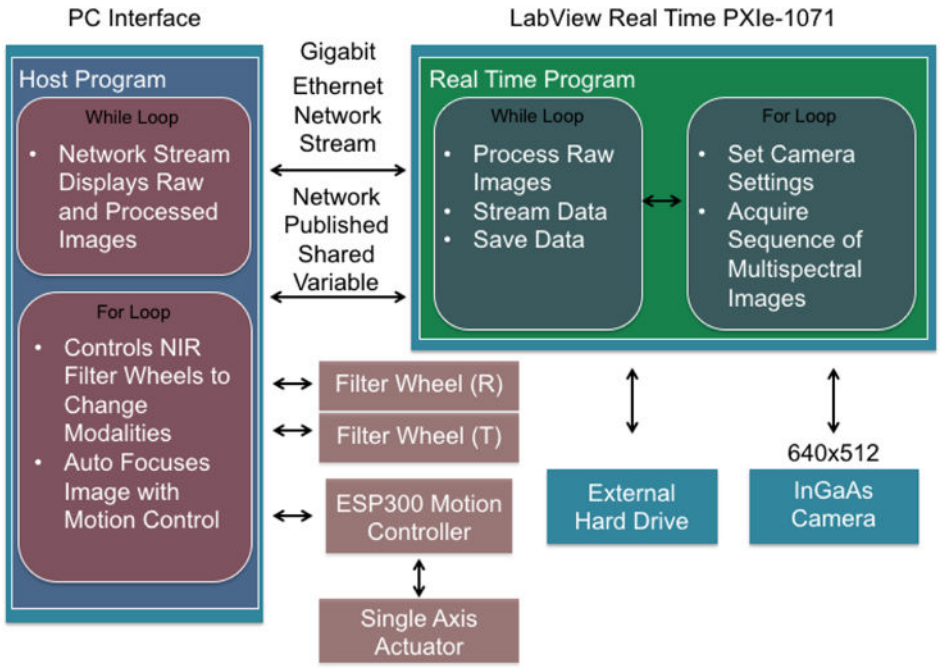

Fig 2.

Computer network schematic for multispectral-multimodal NIR reflectance and occlusal transillumination system. Black arrows represent data communication and external device control. Image acquisition is controlled by the real time PXIe-1071 (green) computer which is responsible for changing the cameras operational settings for each different modality and wavelength in order to optimize image contrast. The image sequence begins with a continuous reflectance acquisition and then acquires a set number of frames/images for the following multispectral modalities. Images are live streamed and viewed on the host computer over a gigabit Ethernet network stream. The real time computer communicates which image modality to acquire to the host using a network published variable.

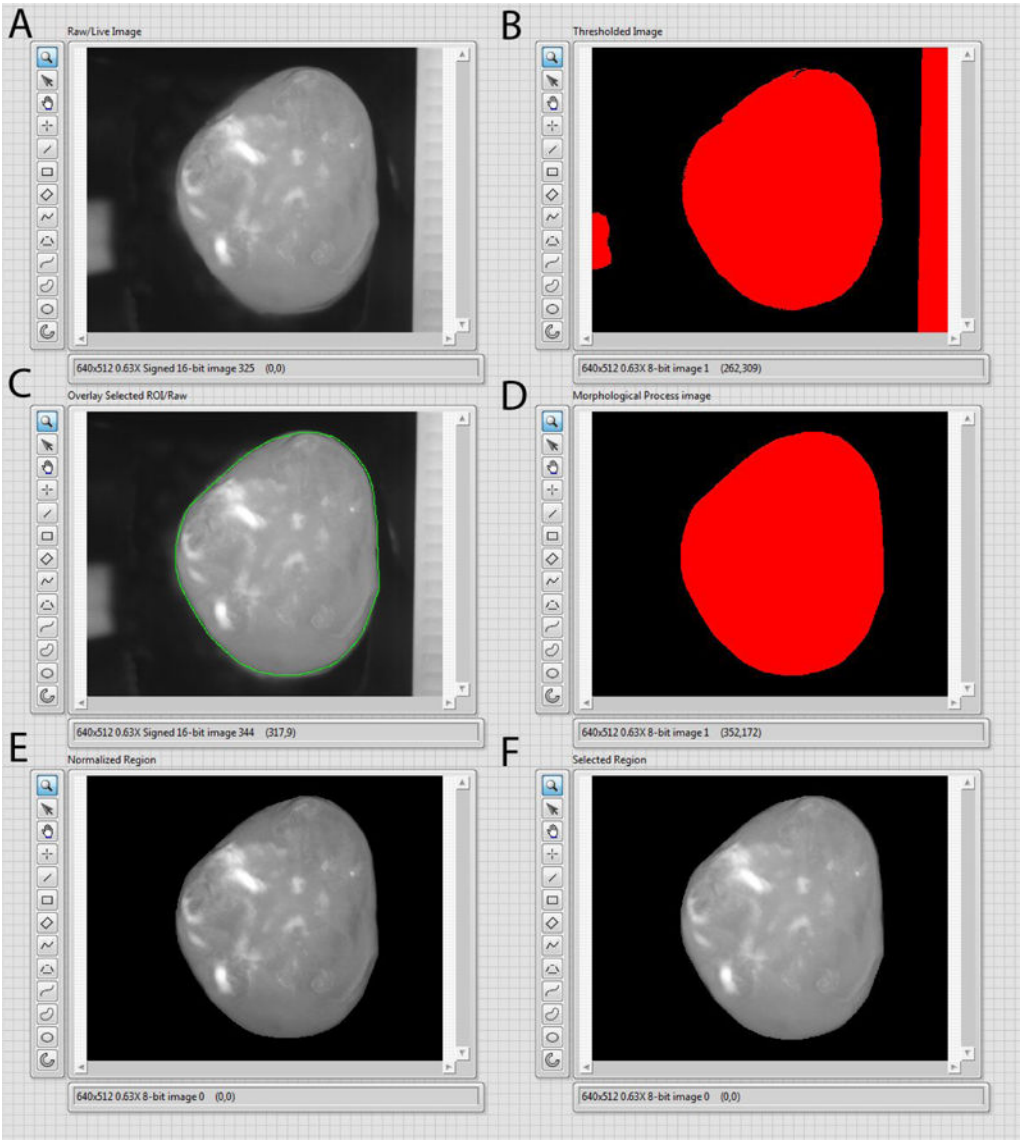

Fig 3.

Cross polarized reflectance image at 830-nm and processing steps for tooth pixel extraction, (A) Raw 830-nm cross polarized reflectance image with object placed to the right of the tooth to demonstrate robustness of isolation, (B) Binary image after statistical thresholding, (C) Overlay of selected pixel region with raw image after morphological processing, (D) Binary image post morphological operations, (E) Normalized tooth image of selected pixels, and (F) Raw tooth image of selected pixels.

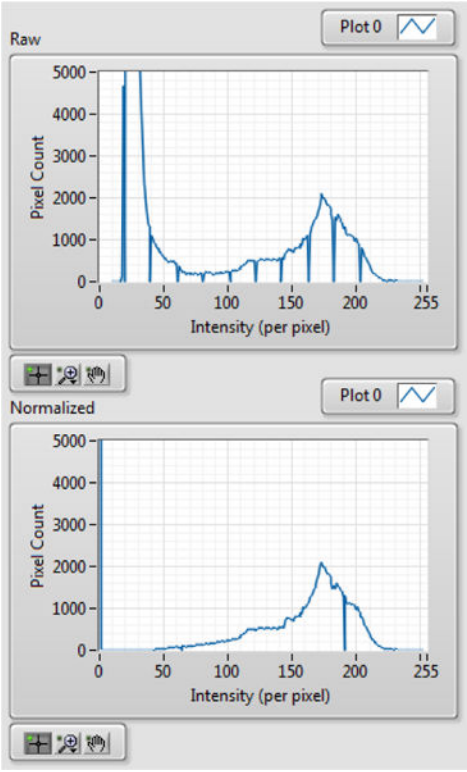

Fig 4.
Histogram of pixel values from the raw (top) and processed/normalized image (bottom).